

Figure 1. Topographic map of Niobe Planitia quadrangle (V-23), Venus, showing major features including highland regions to the south and lowlands to the north. Mercator projection.

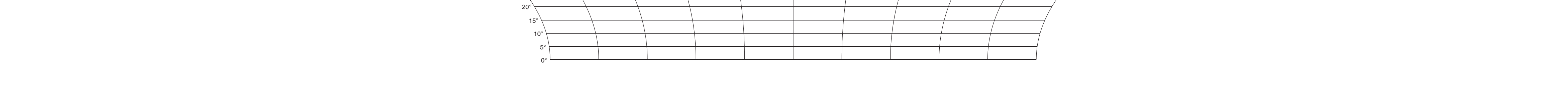


Figure 2. Magellan SAR image showing major features and figure locations in Niobe Planitia quadrangle (V-23), Venus. Mercator projection.

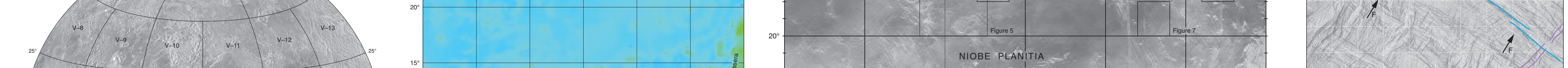


Figure 3. Inverted left-illumination Magellan SAR image showing details of shield terrain and tectonic structures in unit FN, Niobe quadrangle (V-23), Venus. A. Image centered at 22° N, 100.3° E, showing concentric structures in the upper left are part of Mayia Corona that dominantly predates shield-terrain formation; north-northwest-striking fractures and east-northeast-trending wrinkle ridges parallel regionally extensive structural suites. East-striking fractures in the bottom of the image occur within a more localized region. Shields are scattered across the surface. Enlargements B and C show a range of shield morphologies and temporal relations with secondary structures. Black arrows point to a few shields that are well to poorly defined. North-striking regional fractures generally predates shield formation, and reactivation along north-striking fractures locally postdates shield emplacement (white arrows). Dashed lines indicate examples of well-defined (upper C) and more poorly defined (B and lower C) limits of shield deposits; local regions of fracture terrain are exposed as kippas among shield deposits (C).

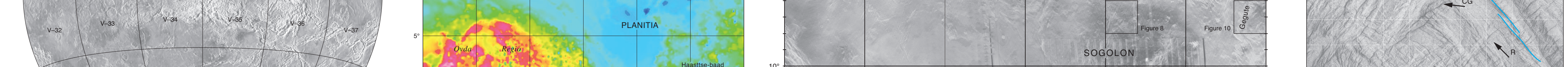


Figure 4. Left-illumination Magellan SAR image of ribbon-tessera terrain (unit rT), illustrating intratessera basin, low viscosity fill (unit rTb), enclosed by dashed lines in local topographic lows, Niobe quadrangle (V-23), Venus. Note that fill contact is locally gradational and locally covers and is cut by both northeast-trending extensional structures (a few highlighted by black lines) and northwest-trending contractional structures. Arrows indicate ribbon (R), fold (F), and complex graben (CG) structures. Several generations of low viscosity fill occur. Many intratessera basins shown here are not visible on the 1:5,000,000-scale map. Intratessera basins tend to parallel fold troughs at all scales, although, locally, northeast-trending extensional troughs are also filled. Map relations clearly indicate that layer extension and layer contraction occurred broadly and synchronously and that flooding of local topographic lows accompanied deformation.

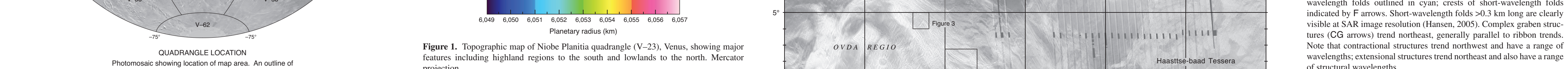


Figure 5. Right-illumination Magellan SAR images cropped from C1- and full-resolution SAR images showing details of shield terrain and tectonic structures in unit FN, Niobe quadrangle (V-23), Venus. A. Image centered at 22° N, 100.3° E, showing concentric structures in the upper left are part of Mayia Corona that dominantly predates shield-terrain formation; north-northwest-striking fractures and east-northeast-trending wrinkle ridges parallel regionally extensive structural suites. East-striking fractures in the bottom of the image occur within a more localized region. Shields are scattered across the surface. Enlargements B and C show a range of shield morphologies and temporal relations with secondary structures. Black arrows point to a few shields that are well to poorly defined. North-striking regional fractures generally predates shield formation, and reactivation along north-striking fractures locally postdates shield emplacement (white arrows). Dashed lines indicate examples of well-defined (upper C) and more poorly defined (B and lower C) limits of shield deposits; local regions of fracture terrain are exposed as kippas among shield deposits (C).



Figure 6. Right-illumination inverted SAR image (A) centered at lat 13° N, long 111° E, showing fracture terrain of Niobe Planitia (unit FN) and locations of enlargements C-E, and mapped geologic structures (B). Niobe quadrangle (V-23), Venus. Geologic structures (B) show definite shields (black crosses), potential shields (gray crosses), wrinkle ridges (gray lines), and fractures (black lines); white background indicates region of shield terrain shown in image A. Although many shields are cut by reactivated north-striking fractures, other shields clearly postdate fracture reactivation (C, arrows). Locally, shield-paint-filled fractures are inverted by layer contraction resulting in north-trending inversion structures: folds or wrinkle ridges (gray lines, B; i arrows, D, E) and open fractures (o arrows, D, E). Open fractures are locally modified along strike, either covered by shield deposits and (or) forming inversion structures (E).

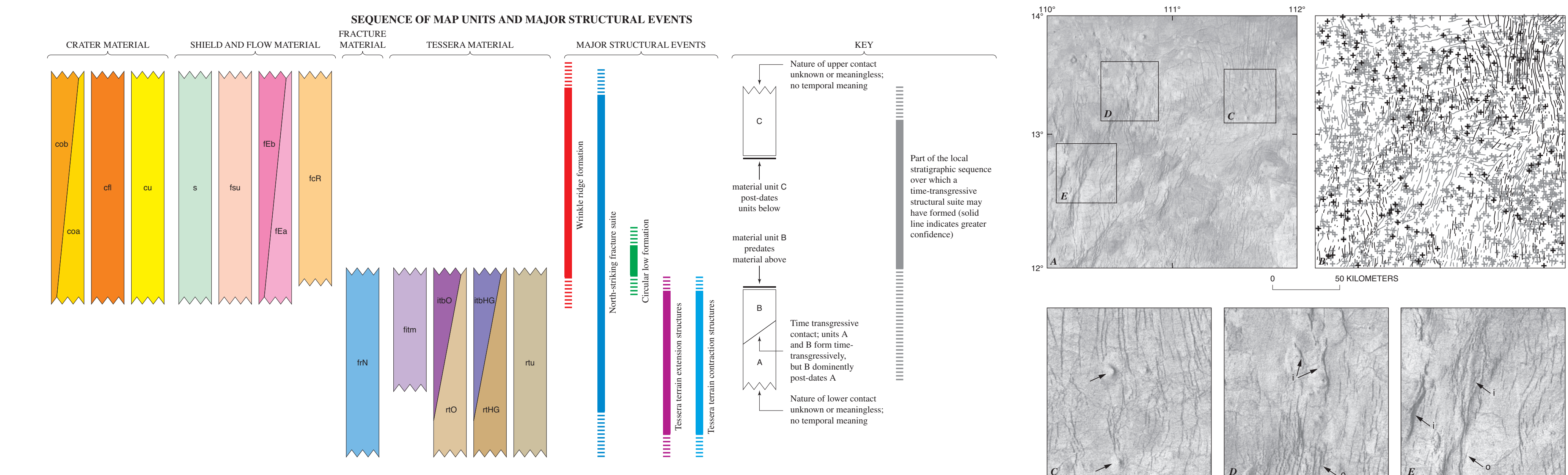


Figure 7. Right-illumination inverted SAR image (A) centered at lat 23° N, long 103° E, showing fracture terrain of Niobe Planitia (unit FN) and locations of enlargements C-E, and mapped geologic structures (B). Niobe quadrangle (V-23), Venus. Geologic structures (B) show definite shields (black crosses), potential shields (gray crosses), wrinkle ridges (gray lines), and fractures (black lines); white background indicates region of shield terrain shown in image A. Although many shields are cut by reactivated north-striking fractures, other shields clearly postdate fracture reactivation (C, arrows). Locally, shield-paint-filled fractures are inverted by layer contraction resulting in north-trending inversion structures: folds or wrinkle ridges (gray lines, B; i arrows, D, E) and open fractures (o arrows, D, E). Open fractures are locally modified along strike, either covered by shield deposits and (or) forming inversion structures (E).

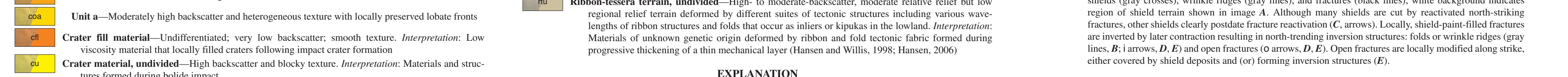


Figure 8. Right-illumination inverted SAR image (A) centered at lat 13° N, long 117° E, showing fracture terrain of Niobe Planitia (unit FN) and locations of enlargements C-E, and mapped geologic structures (B). Niobe quadrangle (V-23), Venus. Geologic structures (B) show definite shields (black crosses), potential shields (gray crosses), wrinkle ridges (gray lines), and fractures (black lines); white background indicates region of shield terrain shown in image A. Ribbon-terrain (shaded dark gray) shows ribbon trends (black lines). Ribbon fabric is highlighted in C, note that shield paint fills topographic lows of detailed ribbon-terrain. Fine-scale polygonal fabric (shaded light gray), open (reactivated?) fractures (o arrows), and inversion structures (i arrows) are apparent in D and E. This region also shows a delicate, closely spaced, northeast-trending lineament fabric (black lines, E).



Figure 9. Right-illumination inverted SAR image (A) centered at lat 23° N, long 117° E, showing fracture terrain of Niobe Planitia (unit FN) and locations of enlargements C-E, and mapped geologic structures (B). Niobe quadrangle (V-23), Venus. Geologic structures (B) show definite shields (black crosses), potential shields (gray crosses), wrinkle ridges (gray lines), and fractures (black lines); white background indicates region of shield terrain shown in image A. Ribbon-terrain (shaded dark gray) shows ribbon trends (black lines). Ribbon fabric is highlighted in C, note that shield paint fills topographic lows of detailed ribbon-terrain. Fine-scale polygonal fabric (shaded light gray), open (reactivated?) fractures (o arrows), and inversion structures (i arrows) are apparent in D and E. This region also shows a delicate, closely spaced, northeast-trending lineament fabric (black lines, E).

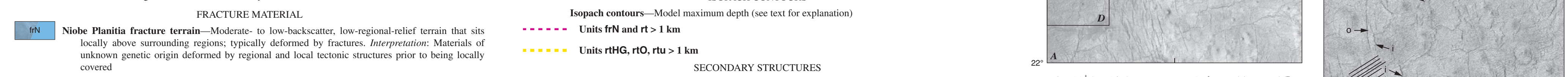


Figure 10. Right-illumination inverted SAR image (A) centered at lat 13° N, long 119° E, showing fracture terrain of Niobe Planitia (unit FN) and locations of enlargements C-E, and mapped geologic structures (B). Niobe quadrangle (V-23), Venus. Geologic structures (B) show definite shields (black crosses), potential shields (gray crosses), wrinkle ridges (gray lines), and fractures (black lines); white background indicates region of shield terrain shown in image A. This region displays a large ribbon-terrain (shaded dark gray) with several small, gently marks older ribbon fabrics (C). The geologic map (B) was constructed using co-registered right- and left-illumination SAR in both normal and inverted modes.



Figure 11. Sketch illustrating the importance of an existing anisotropy in stress-strain relations. A. A layer of corrugated cardboard (lines represent corrugation axes) defines a penetrative structural/mechanical fabric anisotropy. Application of a wide range of orientations of maximum compressive stress (arrows, A to C) results in the same orientation of longer wavelength folds (terrain) with resulting fold axis parallel to the corrugations (B); minimum compressive stress indicated by short line normal to maximum compressive stress axis. The resulting strain is inverted the orientation of the principle stress axes.



Figure 12. Right-illumination inverted SAR image (A) centered at lat 21° N, long 113° E, and mapped geologic structures and fabric (B), both showing fracture terrain of Niobe Planitia (unit FN) and locations of enlargements C, Niobe quadrangle (V-23), Venus. Geologic structures (B) show definite shields (black crosses), potential shields (gray crosses), wrinkle ridges (gray lines), and fractures (black lines); white background indicates region of shield terrain shown in image A. Wrinkle ridges trend east-northeast; fractures strike north-northwest. Well-developed fine-scale polygonal fabric occurs in patches (B, shaded). The boundary between regions displaying and lacking fine-scale polygonal fabric is sharp to gradational (C) and may reflect the relative thickness of shield paint: fine-scale polygonal fabric marks thinner shield paint. North-northwest-striking open fractures that locally cut shields and shield paint (C, arrows) likely represent reactivation of regional north-northwest-striking fractures. An ~15-km-diameter circular depression marks the northeast corner of the area; extremely fine, typically covered fractures concentric to this structure extend ~60–70 km from its center (B, dashed lines).



Figure 13. Right-illumination inverted SAR image (A) centered at lat 21° N, long 113° E, and mapped geologic structures and fabric (B), both showing fracture terrain of Niobe Planitia (unit FN) and locations of enlargements C, Niobe quadrangle (V-23), Venus. Geologic structures (B) show definite shields (black crosses), potential shields (gray crosses), wrinkle ridges (gray lines), and fractures (black lines); white background indicates region of shield terrain shown in image A. Wrinkle ridges trend east-northeast; fractures strike north-northwest. Well-developed fine-scale polygonal fabric occurs in patches (B, shaded). The boundary between regions displaying and lacking fine-scale polygonal fabric is sharp to gradational (C) and may reflect the relative thickness of shield paint: fine-scale polygonal fabric marks thinner shield paint. North-northwest-striking open fractures that locally cut shields and shield paint (C, arrows) likely represent reactivation of regional north-northwest-striking fractures. An ~15-km-diameter circular depression marks the northeast corner of the area; extremely fine, typically covered fractures concentric to this structure extend ~60–70 km from its center (B, dashed lines).



Figure 14. Right-illumination inverted SAR image centered at lat 23° N, long 103° E. (A), showing fracture terrain of Niobe Planitia (unit FN) and locations of enlargements C and D, and mapped geologic structures (B). Niobe quadrangle (V-23), Venus. Relative spacing of wrinkle ridges and shields results in inconclusive temporal relations (A and C); although some shields postdate secondary structures (white arrows), in most cases shields are older than wrinkle ridges or fractures (black arrows), indicating wrinkle ridges dominantly postdate shields. Geologic structures (B) highlight definite shields (black crosses), potential shields (gray crosses), wrinkle ridges (gray lines), and fractures (black lines); white background indicates region of shield terrain shown in image A. Fine-scale polygonal fabric occurs between wrinkle ridges and is best developed away from shield centers where the unit is likely thin (C). Primary shield structures (D) locally cover and, therefore, formed after locally preserved basal layer marked by closely spaced, east-trending, anastomosing lineaments (white arrows).

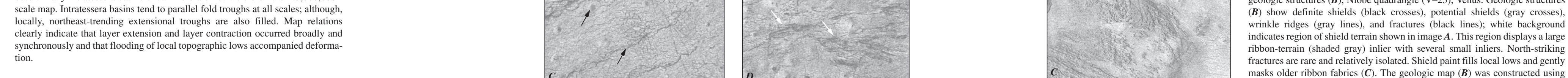


Figure 15. Right-illumination inverted SAR image centered at lat 23° N, long 103° E. (A), showing fracture terrain of Niobe Planitia (unit FN) and locations of enlargements C and D, and mapped geologic structures (B). Niobe quadrangle (V-23), Venus. Relative spacing of wrinkle ridges and shields results in inconclusive temporal relations (A and C); although some shields postdate secondary structures (white arrows), in most cases shields are older than wrinkle ridges or fractures (black arrows), indicating wrinkle ridges dominantly postdate shields. Geologic structures (B) highlight definite shields (black crosses), potential shields (gray crosses), wrinkle ridges (gray lines), and fractures (black lines); white background indicates region of shield terrain shown in image A. Fine-scale polygonal fabric occurs between wrinkle ridges and is best developed away from shield centers where the unit is likely thin (C). Primary shield structures (D) locally cover and, therefore, formed after locally preserved basal layer marked by closely spaced, east-trending, anastomosing lineaments (white arrows).

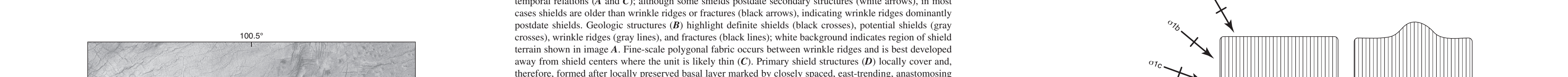


Figure 16. Right-illumination inverted SAR image centered at lat 23° N, long 103° E. (A), showing fracture terrain of Niobe Planitia (unit FN) and locations of enlargements C and D, and mapped geologic structures (B). Niobe quadrangle (V-23), Venus. Relative spacing of wrinkle ridges and shields results in inconclusive temporal relations (A and C); although some shields postdate secondary structures (white arrows), in most cases shields are older than wrinkle ridges or fractures (black arrows), indicating wrinkle ridges dominantly postdate shields. Geologic structures (B) highlight definite shields (black crosses), potential shields (gray crosses), wrinkle ridges (gray lines), and fractures (black lines); white background indicates region of shield terrain shown in image A. Fine-scale polygonal fabric occurs between wrinkle ridges and is best developed away from shield centers where the unit is likely thin (C). Primary shield structures (D) locally cover and, therefore, formed after locally preserved basal layer marked by closely spaced, east-trending, anastomosing lineaments (white arrows).

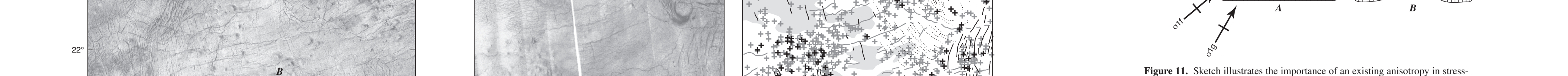


Figure 17. Right-illumination inverted SAR image centered at lat 23° N, long 103° E. (A), showing fracture terrain of Niobe Planitia (unit FN) and locations of enlargements C and D, and mapped geologic structures (B). Niobe quadrangle (V-23), Venus. Relative spacing of wrinkle ridges and shields results in inconclusive temporal relations (A and C); although some shields postdate secondary structures (white arrows), in most cases shields are older than wrinkle ridges or fractures (black arrows), indicating wrinkle ridges dominantly postdate shields. Geologic structures (B) highlight definite shields (black crosses), potential shields (gray crosses), wrinkle ridges (gray lines), and fractures (black lines); white background indicates region of shield terrain shown in image A. Fine-scale polygonal fabric occurs between wrinkle ridges and is best developed away from shield centers where the unit is likely thin (C). Primary shield structures (D) locally cover and, therefore, formed after locally preserved basal layer marked by closely spaced, east-trending, anastomosing lineaments (white arrows).



Figure 18. Right-illumination inverted SAR image centered at lat 23° N, long 103° E. (A), showing fracture terrain of Niobe Planitia (unit FN) and locations of enlargements C and D, and mapped geologic structures (B). Niobe quadrangle (V-23), Venus. Relative spacing of wrinkle ridges and shields results in inconclusive temporal relations (A and C); although some shields postdate secondary structures (white arrows), in most cases shields are older than wrinkle ridges or fractures (black arrows), indicating wrinkle ridges dominantly postdate shields. Geologic structures (B) highlight definite shields (black crosses), potential shields (gray crosses), wrinkle ridges (gray lines), and fractures (black lines); white background indicates region of shield terrain shown in image A. Fine-scale polygonal fabric occurs between wrinkle ridges and is best developed away from shield centers where the unit is likely thin (C). Primary shield structures (D) locally cover and, therefore, formed after locally preserved basal layer marked by closely spaced, east-trending, anastomosing lineaments (white arrows).

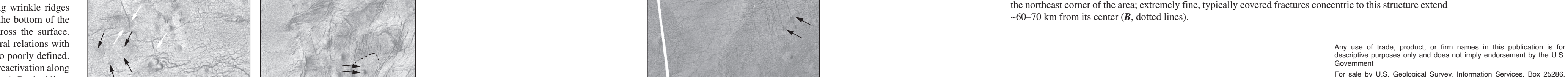


Figure 19. Right-illumination inverted SAR image centered at lat 23° N, long 103° E. (A), showing fracture terrain of Niobe Planitia (unit FN) and locations of enlargements C and D, and mapped geologic structures (B). Niobe quadrangle (V-23), Venus. Relative spacing of wrinkle ridges and shields results in inconclusive temporal relations (A and C); although some shields postdate secondary structures (white arrows), in most cases shields are older than wrinkle ridges or fractures (black arrows), indicating wrinkle ridges dominantly postdate shields. Geologic structures (B) highlight definite shields (black crosses), potential shields (gray crosses), wrinkle ridges (gray lines), and fractures (black lines); white background indicates region of shield terrain shown in image A. Fine-scale polygonal fabric occurs between wrinkle ridges and is best developed away from shield centers where the unit is likely thin (C). Primary shield structures (D) locally cover and, therefore, formed after locally preserved basal layer marked by closely spaced, east-trending, anastomosing lineaments (white arrows).